INT. J. NUM. METH. HEAT FLUID FLOW, VOL. 6 NO. 5, 17–28 (1996)

G-JITTER EFFECTS ON MASS TRANSFER IN ANNULAR LIQUID JETS

J.I. RAMOS

Departamento de Lenguajes y Ciencias de la Computación, E. T. S. Ingenieros Industriales, Universidad de Málaga, Plaza El Ejido, s/n, 29013-Málaga, Spain

ABSTRACT

This paper analyses numerically the effects of sinusoidal g-jitter on the fluid dynamics of, and mass transfer in, annular liquid jets. It is shown that the pressure and volume of the gases enclosed by the jet, the gas concentration at the jet's inner interface, and the mass absorption rates at the jet's inner and outer interfaces are sinusoidal functions of time which have the same frequency as that of the g-jitter. The amplitude of these oscillations increases and decreases, respectively, as the amplitude and frequency, respectively, of the g-jitter is increased. The pressure coefficient and the gas concentration at the jet's inner interface are in phase with the applied g-jitter and the amplitude of their oscillations increases almost linearly with the amplitude of the g-jitter. The mass absorption rates at the jet's inner and outer interfaces exhibit a phase lag with respect to the g-jitter.

KEYWORDS Chemical reactors Annular liquid jets G-jitter Mass absorption

NOMENCLATURE

a = Amplitude of the g-jitter
b = Annular jet's thickness
c = Concentration
C_{pn} = Pressure coefficient
C_{pmax} = Pressure coefficient defined in Eq. (9)
D = Diffusion coefficient
F = Froude number
$\mathbf{F}$ = Flux vector defined in (1)
g = Gravitational acceleration
$\mathbf{G}$ = Vector defined in (1)
H = Henry's constant
J = Defined in (5)
L = Annular jet's convergence length
m = Jet's mass per unit length and per radian, mass
M = Reference mass defined in (16)
p = Pressure
r = Radial co-ordinate
R = Annular jet's mean radius
S = Solubility
St = Strouhal number
t = Time
T = Temperature
u = Mean axial velocity component
$\mathbf{U}$ = Vector of dependent variables defined in (1)
v = radial velocity component
$\bar{v}$ = Average radial velocity component
V = Volume of the gases enclosed by the annular jet
We = Weber number
z = Axial co-ordinate

Greek symbols

α = Non-dimensional constant defined in (23)
β = Non-dimensional constant defined in (23)
γ = Non-dimensional constant defined in (23)
ω = Frequency of the g-jitter
σ = Surface tension
θ = Angle between the jet's mean radius and the symmetry axis

Subscripts

e = Jet's outer radius, gases surrounding the jet
i = Jet's inner radius, gases enclosed by the jet
0 = Nozzle exit, reference conditions

Superscripts

$*$ = Dimensional quantity

0961–5539/96

Received February 1995
Revised September 1995

INTRODUCTION

Annular liquid jets (*Figure 1*) may form enclosed volumes which can be used as chemical reactors for the combustion of toxic or hazardous products, scrubbing of radioactive and non-radioactive materials, etc.[1]. They may also be used to determine the dynamic surface tension of liquids and the diffusivities of sparingly soluble gases in liquids[2,3]. Due to the small binary diffusion coefficients of gases in liquids, the gases enclosed by the annular liquid jet are absorbed by the liquid at very small rates under both steady[4-6] and transient[7] conditions.

If annular liquid jets are employed in micro-gravity environments or aboard spacecraft to determine the diffusivities of gases in liquids, the effects of residual accelerations on the fluid dynamics and mass transfer equations must be accounted for. The sources of residual acceleration range from the effects of the earth's gravity gradient to g-jitter accelerations which include atmospheric drag on the spacecraft, vibrations of compressors, spacecraft attitude motions arising from machinery vibrations, thruster firings, crew motion, etc.[8]. High frequency accelerations are, in general, unimportant compared with the residual motions caused by low frequency accelerations[9].

For experiments carried out aboard spacecraft, the residual acceleration is, in general, three-dimensional. In this paper, however, we neglect the earth's gravity gradient since the convergence length of the annular liquid jets considered here is small compared with the characteristic dimensions of the spacecraft, and we assume that the g-jitter accelerations are axial. These assumptions allow us to consider axisymmetric, annular jets. Furthermore, since the equations which govern the fluid dynamics of annular liquid jets subject to axial g-jitter accelerations in

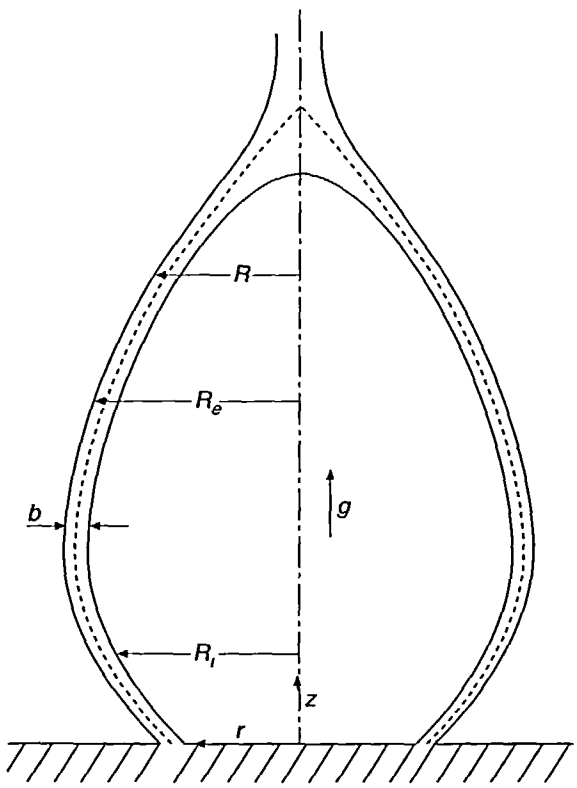

Figure 1 Schematic of an annular liquid jet

inertial frames of reference are analogous to those in noninertial frames which accelerate in a parallel direction to inertial ones, the study presented here is also valid for non-inertial frames of reference, for example the nozzle exit shown in *Figure 1* translates along the z-axis with a time-dependent acceleration. In both cases, the numerical study presented here may be considered as an analysis of the effects of fluctuating body forces on mass transfer phenomena.

G-jitter accelerations may not be periodic functions of time. In this study, however, it is assumed that they are sinusoidal functions of time. Since the equations governing the fluid dynamics of, and mass transfer in, annular liquid jets have been presented elsewhere[5-7,10], only a summary of these equations appears in the next two sections. This summary is aimed at illustrating both the non-linear coupling between linear momentum and mass transfer in time-dependent annular liquid jets, and the effects of g-jitter on the fluid dynamics equations. In the presence or absence of g-jitter, the fluid dynamics and gas concentration equations have been solved numerically by means of a domain-adaptive finite difference method which maps the curvilinear geometry of the jet into a unit square[7,11]. The following section shows the effects of the amplitude and frequency of the g-jitter on the fluid dynamics of and mass transfer in annular liquid jets. The effects of the other non-dimensional parameters which characterize the fluid dynamics and mass transport in annular jets have been the subject of research under both steady[5,6] and transient[7] conditions in the absence of g-jitter, and are not considered here.

FLUID DYNAMICS EQUATIONS

The non-dimensional, asymptotic equations which govern the fluid dynamics of thin, inviscid, incompressible, axisymmetric, annular liquid jets have been derived in Reference 11 by integrating the Euler equations at each cross-section, and by assuming that the pressure is uniform throughout the liquid and that the radial and axial velocity components are not functions of the radial co-ordinate. These equations may be written as

$$\mathbf{U}_t + \mathbf{F}_z = \mathbf{G} \tag{1}$$

where

$$\mathbf{U} = [m, mR, mu, m\bar{v}]^T, \quad \mathbf{F} = [mu, mRu, muu, mu\bar{v}]^T \tag{2}$$

$$\mathbf{G} = \left[0, m\bar{v}, mF + \frac{1}{We}\left(\frac{\partial J}{\partial z} - C_{pn}R\frac{\partial R}{\partial z}\right), \frac{1}{We}\left(C_{pn}R - \frac{\partial J/\partial z}{\partial R/\partial z}\right)\right]^T \tag{3}$$

$$\mathbf{U}(t,0) = [1,\ 1,\ 1,\ \tan\theta_0]^T \tag{4}$$

$$J = R\left/\left[1 + \left(\frac{\partial R}{\partial z}\right)^2\right]^{\frac{1}{2}}\right. \tag{5}$$

$$R_i = R - b/2, \qquad R_e = R + b/2 \tag{6}$$

$$b = R_e - R_i, \qquad R = (R_e + R_i)/2, \qquad b = \frac{m}{R}\frac{b_0^*}{R_0^*} \tag{7}$$

$$F = g^* / u_0^{*2} R_0^*, \qquad We = m_0^* u_0^{*2} / 2\sigma^* R_0^* \tag{8}$$

$$C_{pn} = C_{p\max}\left(\frac{p_i^*}{p_e^*} - 1\right), \qquad C_{p\max} = p_e^* R_0^* / 2\sigma^*, \tag{9}$$

the superscript T denotes transpose; We is the Weber number; m is the annular liquid jet's mass per unit length; u and $\bar{v}$ are the mean axial and radial velocity components of the liquid, respectively;

p is the pressure; R and b are the jet's mean radius and thickness, respectively; t is time; z is the axial co-ordinate; C_{pn} denotes the pressure coefficient; the asterisk denotes dimensional quantities; θ_0 is the angle with which the liquid leaves the nozzle; the subscripts i, e and 0 denote the inner and outer interfaces and the nozzle exit, respectively; and, F is the inverse of the Froude number which is a function of time when there is g-jitter. If the jitter is sinusoidal, i.e.

$$g^* = g_0^*(1 + a\sin(\omega^* t^*)), \tag{10}$$

where g_0^* is the background (constant) gravitational acceleration, and a and ω^* denote the amplitude and frequency of the g-jitter, the inverse of the Froude number may be written as

$$F = F_0(1 + a\sin(2\pi St)), \tag{11}$$

where

$$F = \frac{g_0^*}{R_0^* u_0^{*2}}, \quad St = \frac{\omega^* u_0^*}{2\pi R_0^*}. \tag{12}$$

F_0 denotes the inverse of the Froude number associated with the background gravitational acceleration, and St is the Strouhal number of the sinusoidal g-jitter.

In the above equations, length, time, velocity components and mass per unit length have been non-dimensionalized with respect to R_0^*, R_0^*/u_0^*, u_0^* and $m_0^* = \rho R_0^* b_0^*$, respectively, where ρ^* is the liquid density.

The annular liquid jet merges on the symmetry axis to become a "solid" one at an axial distance $L(t)$ from the nozzle exit which is referred to as the convergence length, and which may be determined from (cf. (6))

$$R_i(t, z = L(t)) = 0, \quad b(t, z = L(t)) = 2R(t, z = L(t)) \tag{13}$$

which implies that (cf. (7))

$$2R^2(t, z = L(t)) = b_0^* \frac{m(t, z = L(t))}{R_0^*}. \tag{14}$$

Equation (14) may be differentiated with respect to t to obtain an ordinary differential equation for L, which accounts for the values of u, $\bar{v}$, R and m and their partial derivatives with respect to z at the convergence point[7,11]. Therefore, the convergence length is non-linearly coupled to the fluid dynamics equations. Furthermore, the volume of the gases enclosed by the annular liquid jet depends on the convergence length. If these gases are assumed to be ideal and isothermal at the temperature $T_i^* = T_e^*$ and consist of a single species, if their pressure and concentration are uniform, and if the Mach number is small, then[7,11]

$$\frac{p_i^*}{p_e^*} = \frac{m_i}{V}, \quad V = \int_0^L R_i^2 dz \tag{15}$$

where

$$m_i = m_i^*/M_i^*, M_i^* = \pi R_0^{*3} p_e^*/\tilde{R}T_i^*. \tag{16}$$

$\tilde{R}$ is the specific gas constant, and V is the non-dimensional volume of the gases enclosed by the annular liquid jet. The assumption of uniform pressure throughout the volume enclosed by the annular liquid jet can be justified if the Mach number is small, while the assumption of a uniform concentration is based on the fact that the mass diffusivities of gases are much higher than the binary diffusion coefficients of gases in liquids.

The gases surrounding the liquid jet are assumed to be ideal, isothermal, single component, identical to those enclosed by the jet and infinite in extent so that p_e^* can be assumed to be constant.

Equations (1) and (15) indicate that the fluid dynamics of annular liquid jets depend on m_i which, in turn, depends on the mass absorbed by the liquid and on the mass injected into and/or the mass generated in the volume enclosed by the jet. In the absence of mass injection or mass generation, m_i depends on the mass absorbed by the liquid as determined in the following sections.

GAS CONCENTRATION IN THE ANNULAR LIQUID JET

If volumetric displacement effects due to the gas absorbed by the liquid are small, the liquid may be assumed to be incompressible, and if the interfaces are clean, mass transfer resistances can be neglected. Under these conditions, the gas concentration at the jet's interfaces is determined from equilibrium conditions corresponding to Henry's solubility law, and the gas concentration in the liquid is governed by the following non-dimensional equations[5-7,11].

$$\frac{\partial u}{\partial z}+\frac{1}{r}\frac{\partial}{\partial r}(rv)=0 \tag{17}$$

$$\frac{\partial c}{\partial t}+u\frac{\partial c}{\partial z}+v\frac{\partial c}{\partial r}=\frac{1}{Pe}\left[\frac{1}{r}\frac{\partial}{\partial r}\left(r\frac{\partial c}{\partial r}\right)+\frac{\partial^2 c}{\partial z^2}\right] \tag{18}$$

$$c(t,r,0)=\alpha(\beta-1), \quad R_i(t,0)<r<R_e(t,0) \tag{19}$$

$$c(t,R_i(t,z),z)=\alpha\left[\gamma\frac{m_i}{\int_0^L R_i^2\,dz}-1\right] \tag{20}$$

$$c(t,R_e(t,z),z)=0 \tag{21}$$

$$u\frac{\partial c}{\partial z}+v\frac{\partial c}{\partial r}=0, \quad \text{at } z=L(t) \tag{22}$$

$$Pe=u_0^*R_0^*/D^*,\ \alpha=2\tilde{R}T_i^*S_e^*,\ \beta=c_0^*/S_e^*p_e^*,\ \gamma=S_i^*/S_e^*=H_e^*/H_i^*, \tag{23}$$

where Pe is the Peclet number; $S_i^*=H_i^{*-1}$ and $S_e^*=H_e^{*-1}$ denote the solubilities at the annular jet's inner and outer surfaces, respectively; H_i^* and H_e^* denote the Henry constants at the annular jet's inner and outer interfaces, respectively; D^* is the diffusivity of the gas in the liquid; and, c_0^* is the dimensional gas concentration at the nozzle exit.

The radial velocity component which appears in (18) may be calculated by integrating (17) from $R_i(t,z)$ to r and using the condition that the annular liquid jet's inner interface is a material surface, as

$$vr=R_i\frac{\partial R_i}{\partial t}-\frac{\partial}{\partial z}\left[u\frac{r^2-R_i^2}{2}\right] \tag{24}$$

where u has been assumed to be only a function of t and z. This assumption can be justified, for the gases surrounding and enclosed by the jet have much smaller densities and dynamic viscosities than those of the liquid and, therefore, they cannot introduce strong velocity variations across the annular jets. This assumption is not, however, valid near the nozzle exit, where the liquid relaxes from stick boundary conditions at the nozzle walls to slip/free boundary conditions at the jet interfaces[10]. It is also not valid near the convergence point, i.e. near $z = L$, where a

meniscus and an axial pressure gradient may exist. Axial and radial pressure gradients were neglected in the derivation of (1)[10].

The non-dimensional mass transfer rate at the inner interface can be written as[5-7,11]

$$\frac{dm_i}{dt} = \frac{1}{Pe}\int_0^L R_i \frac{\partial c}{\partial r}(t, R_i(t,z), z)(1+\tan^2\theta_i)dz \tag{25}$$

subject to

$$m_i(0) = \frac{p_i^*(0)}{p_e^*}\int_0^L R_i^2(0,z)dz \tag{26}$$

where (15) has been used, and

$$\tan\theta_i = \frac{\partial R_i}{\partial z}. \tag{27}$$

A similar expression may be derived for the non-dimensional mass flux at the outer surface of the annular jet.

The integrodifferential Equations (1), (15), (18) and (25) indicate that, in the absence of both mass injection into and mass generation in the volume enclosed by the annular liquid jet, its fluid dynamics depends on b_0^*/R_0^*, $C_{p\max}$, Pe, α, β, γ, F_0, a, St, We, θ_0 and $p_i^*(0)/p_e^*$. Note that, under

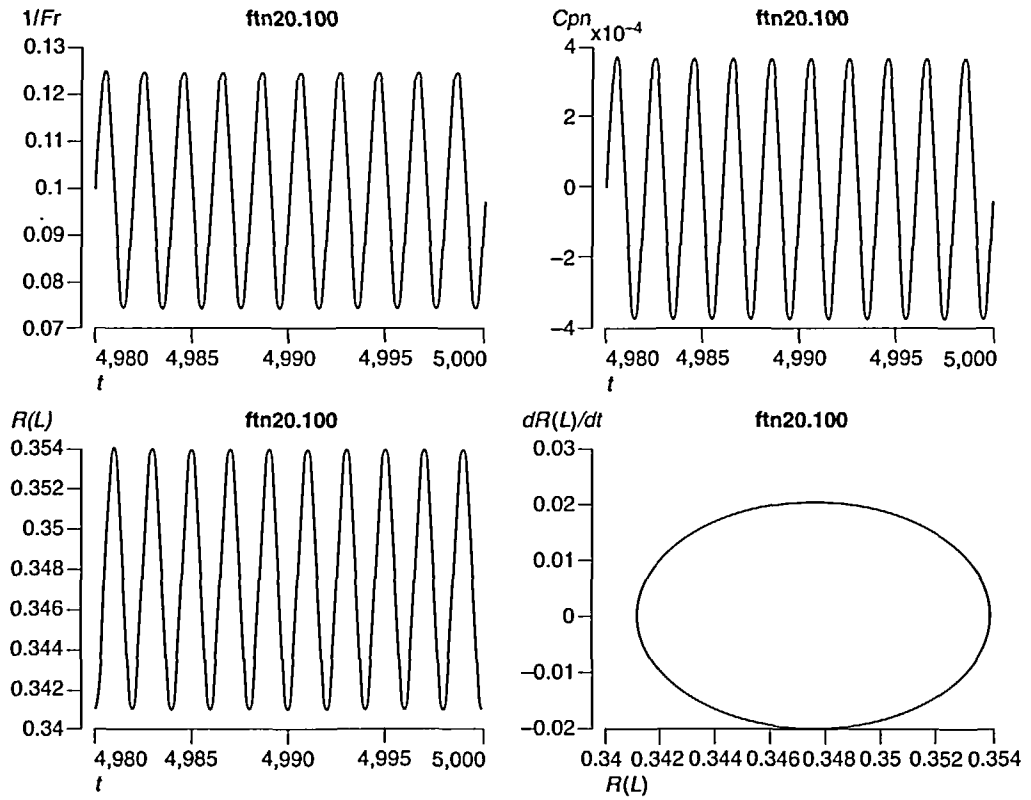

Figure 2 Inverse of the Froude number (top left), pressure coefficient (top right), and jet's mean radius at the convergence point (bottom left) as functions of time, and phase diagram for the jet's mean radius at the convergence point (bottom right)

steady state conditions, the convergence length is constant and the fluid dynamics equations are uncoupled from mass transfer phenomena.

PRESENTATION OF RESULTS

As shown in the second section, the fluid dynamics of, and the mass absorption by, annular liquid jets depend on several dimensionless parameters. The values of the parameters used in this paper are : $Pe = 10^5$, $Fr = 10$, $We = 10$, $b_0^*/R_0^* = 0.05$, $\theta_0 = 0$, $\alpha = \beta = \gamma = 1$, $C_{p\max} = 1$, and $p_i^*(0)/p_e^*(0) = 0.75$. The values of a and S_t were varied in order to assess the effects of the amplitude and frequency of the g-jitter on mass transfer as indicated in the following paragraphs.

All the calculations presented in this paper were performed in double precision arithmetic with an adaptive numerical method which maps the curvilinear geometry of the annular liquid jet into a unit square[7,11]. Initially, $a = 0$ and mass was injected into the volume enclosed by the annular liquid jet at a rate equal to the mass absorption rate by the liquid. Once a steady state was reached, time and the mass injection rate into the volume enclosed by the annular liquid jet were set to zero, and the g-jitter was applied.

The time and spatial steps sizes were varied to ensure that the calculations were grid- and time-step independent. It was observed that $\Delta t = 0.004$ and $\Delta z = 0.04$ gave good results for the g-jitter considered in this paper. Some sample results are presented in *Figures 2-7*.

Figures 2 and *3* correspond to $a = 0.25$ and $S_t = 0.5$, and indicate that the pressure coefficient, the annular liquid jet's mean radius, the volume enclosed by the annular liquid jet, the mass

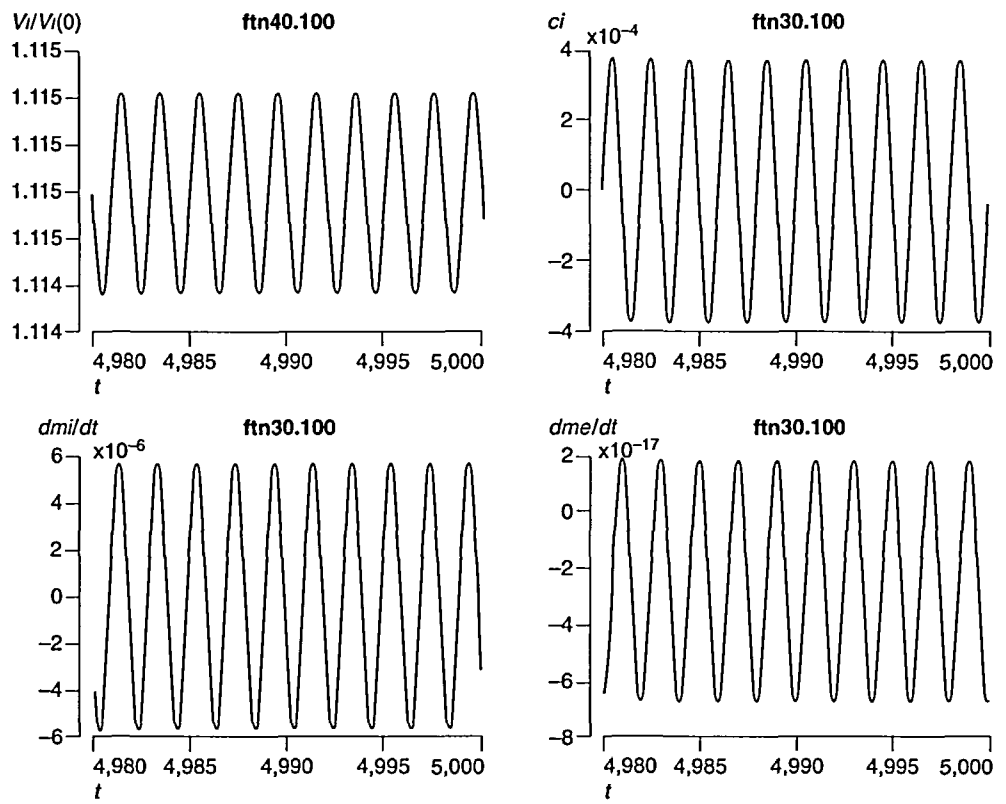

Figure 3 Volume enclosed by the annular liquid jet (top left), gas concentration at the jet's inner interface (top right), and mass absorption rates at the jet's inner (bottom left) and outer (bottom right) interfaces as functions of time

absorption rates at the jet's inner and outer interfaces, and the gas concentration at the jet's inner interface are sinusoidal functions of time and have the same frequency as that of the g-jitter. The pressure coefficient, mass absorption rates, and gas concentration at the jet's inner interface oscillate around a mean value of zero after a long time.

Under steady state conditions, the gas concentrations at the jet's inner and outer interfaces (cf. Eqs. (20) and (21)) are –0.25 and 0, respectively, for the values of the parameters employed in this paper. Therefore, once mass injection into the volume enclosed by the jet is stopped, p_i^* increases until the pressure coefficient, the gas concentration at the jet's inner interface, and the mass transfer rate are zero in the absence of g-jitter. In the presence of g-jitter, one should expect that the pressure of the gases enclosed by the jet and the gas concentration at the jet's inner interface increase in an oscillatory manner until a periodic state is reached. This explains why the results shown in *Figures 2* and *3* oscillate around a mean value of zero.

Figures 2 and *3* also indicate that the pressure coefficient and the gas concentration at the jet's inner interface are in phase with the inverse of the Froude number, whereas there is a phase lag between the applied g-jitter, the jet's mean radius at the convergence point, the volume enclosed by the jet, and the mass absorption rates at the jet's interfaces.

Figures 4 and *5* correspond to $a = 0.75$ and $S_t = 0.5$, and exhibit the same trends as *Figures 2* and *3*. However, the amplitude of the oscillations increases as a is increased, and the phase diagram for the jet's radius at the convergence point becomes more distorted as a is increased. In particular, the amplitude of the oscillations in the pressure coefficient, gas concentration at the

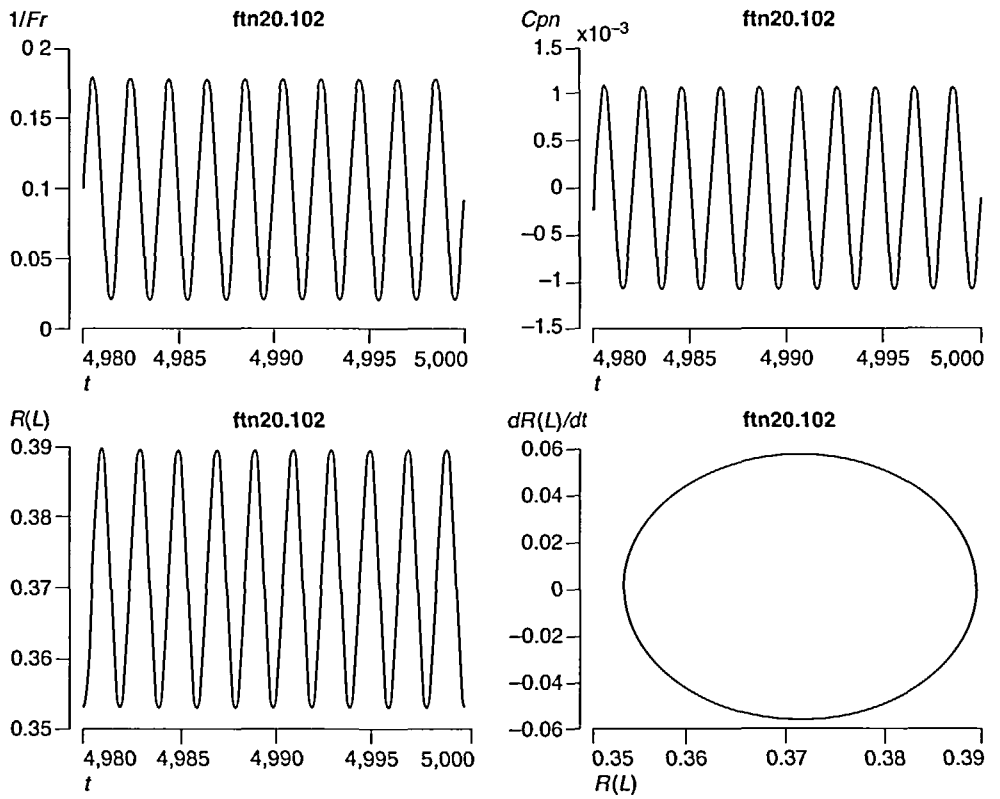

Figure 4 Inverse of the Froude number (top left), pressure coefficient (top right), and jet's mean radius at the convergence point (bottom left) as functions of time, and phase diagram for the jet's mean radius at the convergence point (bottom right)

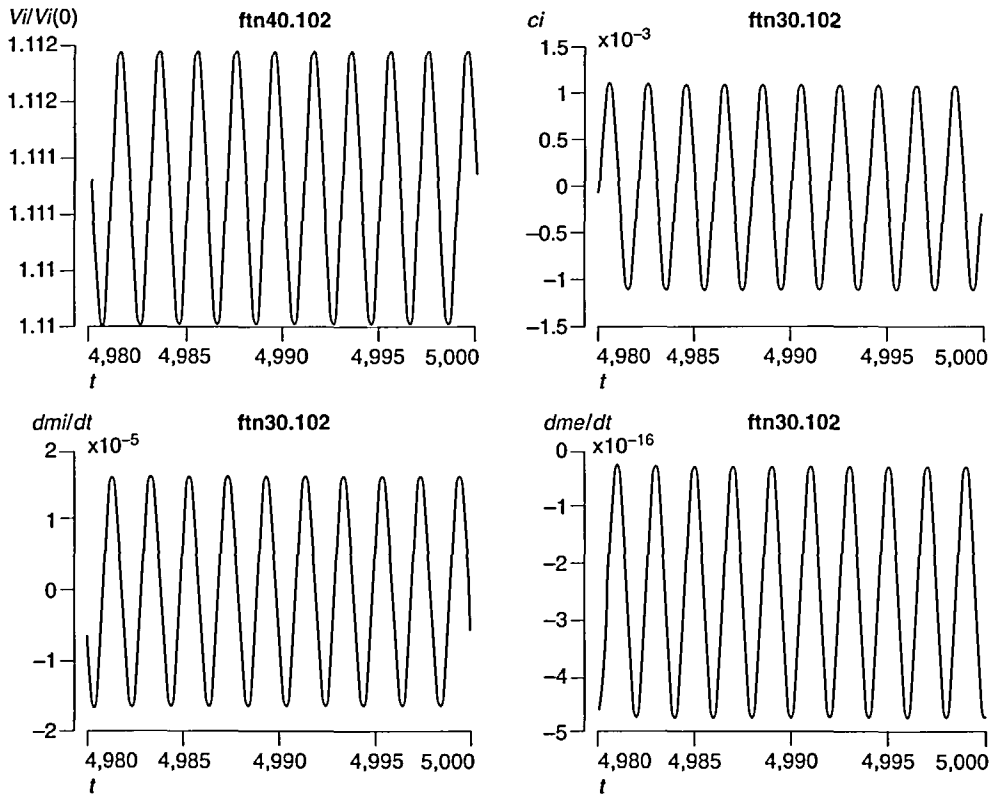

Figure 5 Volume enclosed by the annular liquid jet (top left), gas concentration at the jet's inner interface (top right), and mass absorption rates at the jet's inner (bottom left) and outer (bottom right) interfaces as functions of time

jet's inner interface and mass absorption rates are about three times as large as those of *Figures 2* and *3*, i.e. they increase proportionally to the amplitude of the g-jitter.

Figures 6 and *7* correspond to $a = 0.75$ and $S_t = 1$, and show similar trends to those of *Figures 4* and *5*. However, the amplitude of the oscillations decreases as S_t is increased. For example, for $a = 0.75$ and $S_t = 5$, the amplitude of the oscillations in the pressure coefficient, mass absorption rates at the inner interface, and gas concentration at the jet's inner interface are about 3×10^{-5}, 1.2×10^{-5}, and 3×10^{-5}, respectively.

The results presented in *Figures 2-7* indicate that the mean values of the mass absorption rates at the jet's inner and outer interfaces are zero. Therefore, the non-linear coupling between the fluid dynamics and gas concentration equations does not result in enhanced mass transfer phenomena in environments with gravitational fluctuations. This may be justified in view of the fact that mass transfer in annular liquid jets is a slow phenomenon on account of the small binary mass diffusivities of gases in liquids. Therefore, on the time scale of mass transfer, the average value of the applied sinusoidal g-jitter is zero. This result is consistent with the analytical and numerical, steady state studies presented in References 5, 6 and 11, which show that the convergence length does not increase much as the Froude number is varied.

Although not shown here, the jet's thickness and the axial velocity component at the convergence point are also sinusoidal functions of time.

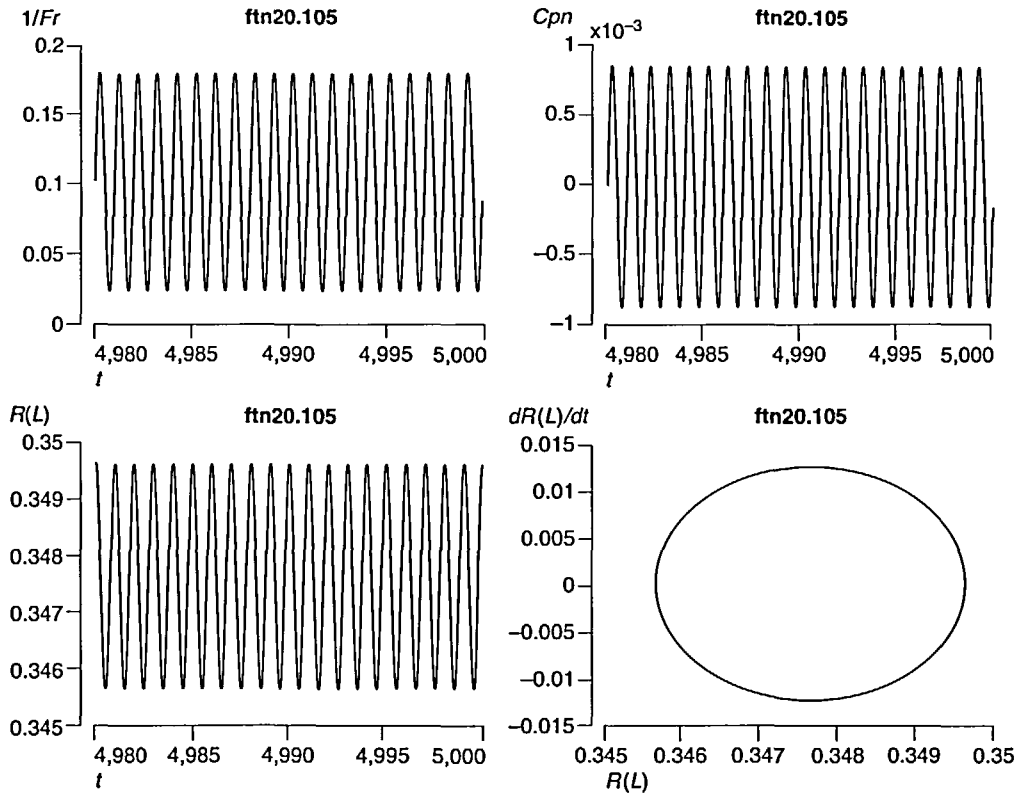

Figure 6 Inverse of the Froude number (top left), pressure coefficient (top right), and jet's mean radius at the convergence point (bottom left) as functions of time, and phase diagram for the jet's mean radius at the convergence point (bottom right)

Figure 8 shows the pressure coefficient, the annular jet's thickness and mean radius at the convergence point, and the mass absorption rate at the jet's inner interface as functions of the amplitude of the g-jitter. This figure clearly summarizes the results of the large number of numerical experiments which have been performed on annular liquid jets subject to g-jitter, and indicates that the pressure coefficient, the annular jet's thickness and mean radius at the convergence point, and the mass absorption rate at the jet's inner interface increase almost linearly as the amplitude of the g-jitter is increased, whereas they decrease as its frequency is increased. The almost linear variations of the results presented in Figure 8 show that, for the amplitudes and frequencies of the g-jitter considered here, the dynamic response of annular liquid jets with mass transfer is a linear phenomenon. Therefore, for the conditions analysed in this paper, the g-jitter does not result in enhanced mass transfer phenomena between the gases enclosed by the annular liquid jet and the liquid.

CONCLUSIONS

The effects of sinusoidal g-jitter on the fluid dynamics of, and mass transfer in, annular liquid jets have been analysed numerically. It has been shown that, despite the non-linear coupling between

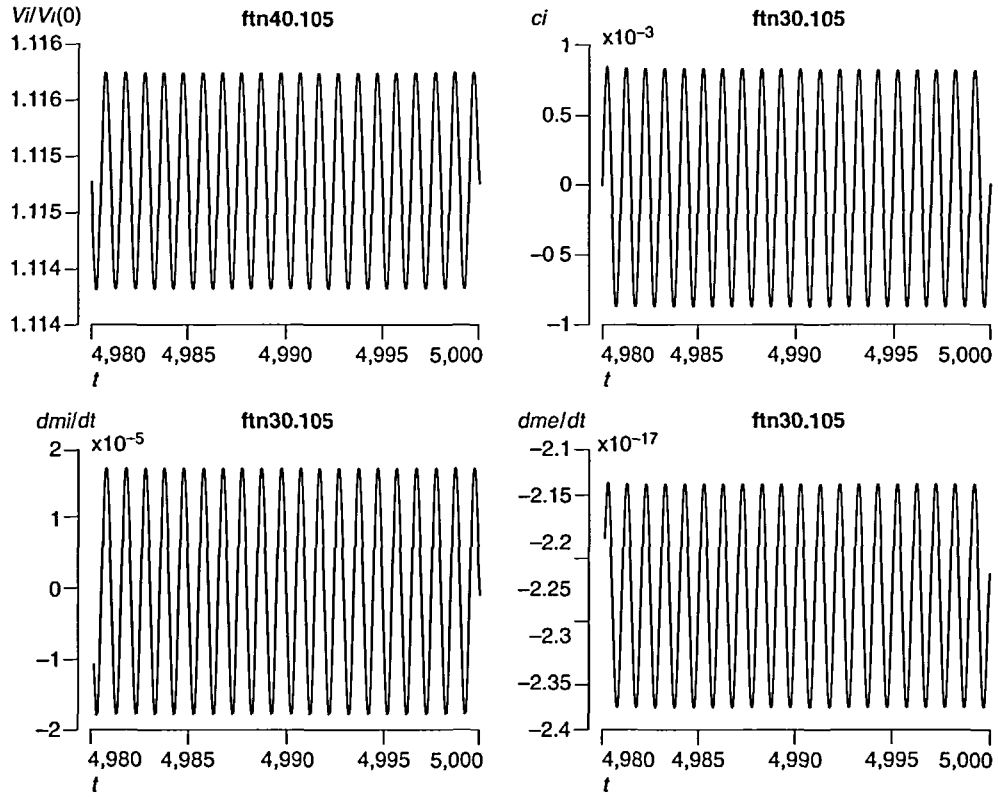

Figure 7 Volume enclosed by the annular liquid jet (top left), gas concentration at the jet's inner interface (top right), and mass absorption rates at the jet's inner (bottom left) and outer (bottom right) interfaces as functions of time

the fluid dynamics and gas concentration equations, the pressure and volume of the gases enclosed by the jet, the gas concentration at the jet's inner interface, and the mass absorption rates at the jet's inner and outer interfaces are sinusoidal functions of time with the same frequency as that of the g-jitter. The amplitude of these oscillations increases and decreases, respectively, as the amplitude and frequency, respectively, of the g-jitter is increased. The mean value of these oscillations is zero owing to the slowness of mass transfer phenomena in gas-liquid systems.

As regards the amplitudes and frequencies considered in this paper, g-jitter does not result in enhanced mass transfer. In fact, it has been observed that the pressure coefficient and the gas concentration at the jet's inner interface are in phase with the applied g-jitter, and the amplitude of their oscillations increases almost linearly with the amplitude of the g-jitter. The mass absorption rates at the jet's inner and outer interfaces exhibit a phase lag with respect to the g-jitter.

ACKNOWLEDGEMENTS

The research reported in this paper was supported by Projects PB91-0767 and PB94-1494 from the DGICYT of Spain.

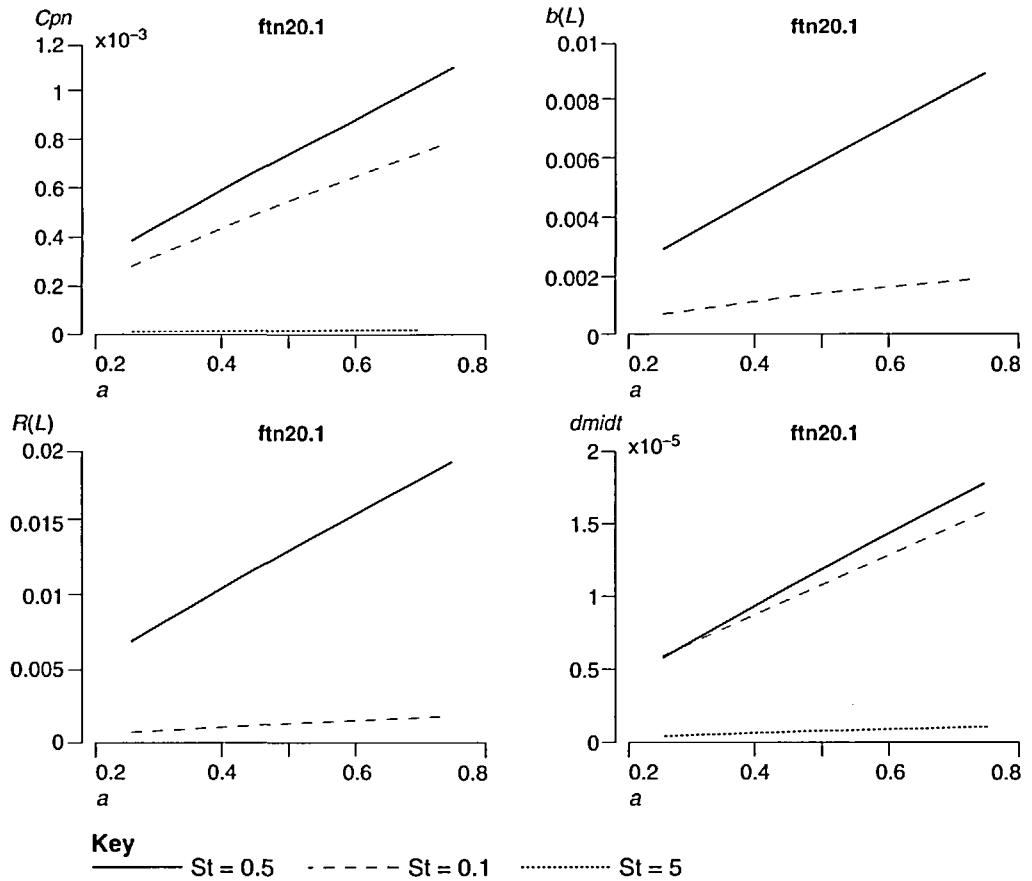

Figure 8 Pressure coefficient (top left), annular jet's thickness at the convergence point (top right), jet's mean radius at the convergence point (bottom left) and mass absorption rate at the jet's inner interface (bottom right) as functions of the amplitude of the g-jitter

REFERENCES

1 Roidt, R.M. and Shapiro, Z.M. *Liquid Curtain Reactor*, Report No.-85M981, Westinghouse R &D Center, Pittsburgh, Pennsylvania (1985)
2 Baird, M.H.I. and Davidson, J.F. Annular jets-I. Fluid dynamics, *Chemical Engineering Science*, **17**, 467-472 (1962)
3 Baird, M.H.I. and Davidson, J.F. Annular jets-II. Gas absorption, *Chemical Engineering Science*, **17**, 473-480 (1962)
4 Ramos, J.I. and Pitchumani, R. Liquid curtains-II. Gas absorption, *Chemical Engineering Science*, **45**, 1595-1604 (1990)
5 Ramos, J.I. Mass absorption by annular liquid jets: I. Analytical and numerical studies using the von Mises transformation, *International Journal of Numerical Methods for Heat & Fluid Flow*, **1**, 99-120 (1991)
6 Ramos, J.I. Mass absorption by annular liquid jets: II. Analytical and numerical studies using a linear mapping, *International Journal of Numerical Methods for Heat & Fluid Flow*, **1**, 121-141 (1991)
7 Ramos, J.I. Mass absorption by annular liquid jets: III. Numerical studies of jet collapse, *International Journal of Numerical Methods for Heat & Fluid Flow*, **2**, 21-36 (1992)
8 Avduyevsky, V.S. editor, *Scientific Foundations of Space Manufacturing*, MIR, Moscow, USSR (1984)
9 Kamotani, Y., Prasad, A. and Ostrach, S. Thermal convection in an enclosure due to vibrations aboard a spacecraft, *AIAA Journal*, **19**, 511-516 (1981)
10 Ramos, J.I. Annular liquid jets: formulation and steady state analysis, *Zeitschrift für Angewandte Mathematik und Mechanik (ZAMM)*} **72**, 565-589 (1992)
11 Ramos, J.I. Domain-adaptive finite difference methods for collapsing annular liquid jets, *Computational Mechanics: An International Journal*, **11**, 28-64 (1993)